Fuzzy Image Processing in Sun Sensor

Sohrab Mobasser, Carl Christian Liebe, and Ayanna Howard
Jet Propulsion Laboratory
California Institute of Technology
4800 Oak Grove Dr, Pasadena, CA 91109, USA
Email: sohrab.mobasser, carl.c.liebe, ayanna.m.howard @jpl.nasa.gov

Abstract

Sun sensors are widely used in spacecraft attitude determination subsystems to provide a measurement of the sun vector in spacecraft coordinates. At the Jet Propulsion Laboratory, California Institute of Technology, there is an ongoing research activity to utilize Micro Electro Mechanical Systems (MEMS) processes to develop a smaller and lighter sun sensor for space applications. A prototype sun sensor has been designed and constructed. It consists of a piece of silicon coated with a thin layer of chrome, and a layer of gold with hundreds of small pinholes, placed on top of an image detector at a distance of less than a millimeter. Images of the sun are formed on the detector when the sun illuminates the assembly. Software algorithms must be able to identify the individual pinholes on the image detector and calculate the angle to the sun. Fuzzy image processing is utilized in this process. This paper will describe how the fuzzy image processing is implemented in the instrument. Comparison of the Fuzzy image processing and a more conventional image processing algorithm is provided and shows that the Fuzzy image processing yields better accuracy then conventional image processing.

I. INTRODUCTION

Future micro/nano spacecraft and rovers will carry sun sensors to determine the pointing direction towards the sun and for position determination. Conventional sun sensors are typically too large compared to the size of a micro/nano spacecraft or a small rover.

Two categories of conventional sun sensors exist - digital and analog types. The digital sun sensor illuminates different geometric pattern on the detector plane. The presence or absence of light imaged on the plane defines a digital signal that can be translated into the sun angle. In comparison, an analog sun sensor outputs analog currents, from which the sun angles can be derived directly [1].

To enhance the capabilities of these traditional sun sensor devices, a new generation of sun sensors is emerging. These sun sensors utilize an imaging device as the detector plane with a mask placed in front of it. The sun sensor determines sun angles based on the location of the image pattern on the detector plane [2], [3], and [4].

At the Jet Propulsion Laboratory, California Institute of Technology, there is currently an ongoing multi-year research task to miniaturize sun sensors utilizing MEMS technology. A number of masks with different patterns have been developed. These MEMS masks were manufactured using a 500-micron thick silicon wafer. The mask placed on top of an Active Pixel Sensor (APS) image detector basically functions as the entire sensor [5].

This paper describes the Fuzzy image-processing algorithm used to determine the sun angle. The experimental results and calibrations are also included. A comparison of the Fuzzy image processing and a more conventional image processing method of angle determination is also provided.

II. MEMS BASED SUN SENSOR

The key components of this highly accurate and very small sun sensor are the high-resolution multi aperture mask and a novel Fuzzy image processing. The basic concept is shown in Figure 1.

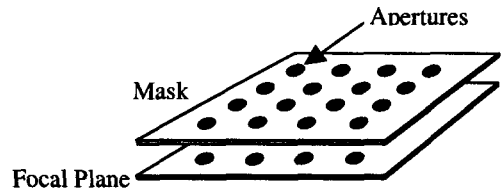

Figure 1: MEMS sun sensor principle

The size of a focal plane is 6.1 mm x 6.1 mm and the size of the individual pixels is 12 microns. It is assumed that the accuracy of the sun sensor is proportional to the square root of the number of apertures. Therefore, it is desired to have a large number of apertures.

The masks were fabricated from a 6-inch diameter by 500-micron thick silicon wafer. The size of each mask is 7 mm x 7 mm. Six different combinations of aperture diameters and aperture spacing were manufactured (apertures: 16, 32 and 64 microns and aperture spacing: 128 and 256 microns). Figure 2 shows a sketch of the mask patterns. In Figure 3 a photograph of a MEMS mask is shown. One side is the raw silicon. The other side is gold coated. The pinholes in the gold coating are to small to be seen in this photograph

An Active Pixel Sensor (APS) chip is used as an image detector [5]. The chip is a camera with all functions (such as A/D conversion, photosensitive area, control logic etc.) embedded on the device.

III. FUZZY IMAGE PROCESSING

In an image captured from the MEMS sun sensor, a pattern of approximately 300 equally spaced apertures is observed as shown in Figure 4. The position of this pattern on the focal plane changes as a function of the sun angles.

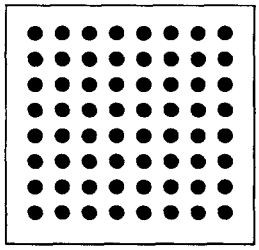

Figure 2: Sketch of a MEMS mask

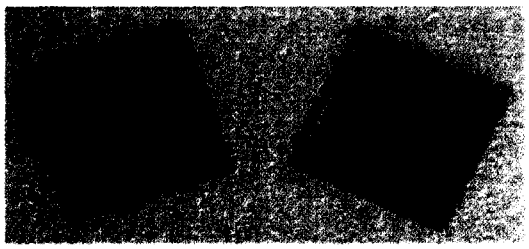

Figure 3: Photograph of MEMS mask

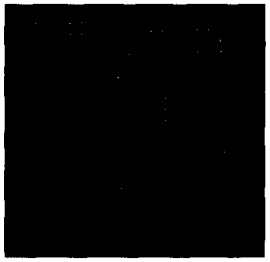

Figure 4: Typical image from the sun sensor

Typically, pixels that have a brightness value above a given threshold are detected within an image and used to extract centroid information. The problem, utilizing a static threshold value, is that the resulting pattern on the detector is not consistent, depending on the angle of the sun. In some cases, we get a perfectly imaged pattern in which we can correctly extract centroid information using the algorithm defined in the previous section. In other cases, we get highly contrasting streaks of light in which pixel centroids are blended together. Figure 5 shows an example of a pattern that is difficult to perform the thresholding operation for determining individual centroids.

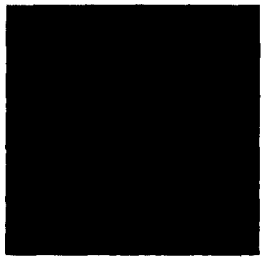

Figure 5: Sun sensor image acquired at a large angle

To resolve this issue, our approach for thresholding has been to use a robust threshold calculation method based on fuzzy-logic rule sets.

Fuzzy Logic is a mechanism for formulating and transferring human expert knowledge into real world applications. Fuzzy logic [6] provides a flexible tool for modeling the relationship between input and output information and is distinguished by its robustness with respect to noise and variations in system parameters. Linguistic fuzzy sets and conditional statements allow systems to make decisions based on imprecise and incomplete information. As such, linguistic fuzzy sets can be used to automatically find threshold values based on characteristics of the image itself.

Based on examples of imaged masks, we have noted that two main factors contribute to differences in the type of images formed: 1) location of mask center and 2) number of non-dark pixels images in mask. For example, given a perfectly imaged mask we find that the threshold required is directly equivalent to the average pixel value of all non-dark pixels. From this reference point, we recognize that if an image is streaky and thus has more non-dark pixels than the reference case, then we want a threshold value higher than the average in order to remove as many unwanted pixels as possible. Based on this mode of thought, we can represent the two image characteristics as *Mask_Center* and *Num_Non-Dark_Pixels* using linguistic-based variables. We represent *Mask_Center* using the linguistic fuzzy sets {LEFT, CENTER, RIGHT} and Num_Non-Dark_Pixels using the linguistic fuzzy sets {LOW, MED, HIGH}. This is shown in Figure 6.

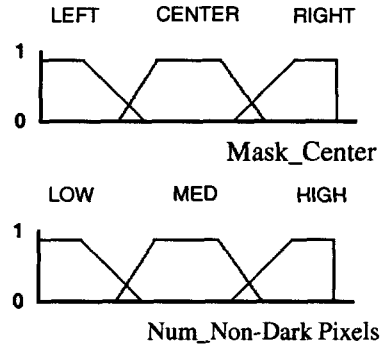

Figure 6: Fuzzy sets for image characteristics

Given the two image characteristics, we robustly calculate the threshold value by increasing the threshold value calculated for the reference case by a dynamic multiplication factor.

$$Thresh = Mult\_Factor * \frac{\sum_{i=0}^{N} p_i}{N} \quad (1)$$

where p_i is the image pixel value, N is the total number of non-dark pixels, *Mult_Factor* is a dynamic multiplication factor, and *Thresh* is the calculated threshold value.

The multiplication factor is dynamic and based on current image characteristics. Thus, the multiplication factor is characterized by the linguistic fuzzy set {LOW, MED, HIGH} and is inferred using a fuzzy rule base with a typical rule as follows:

IF *Mask_Center* **is Centered** and *Num_Non-Dark_Pixels* **is Medium,**
THEN *Mult_Factor* **is Medium**

The final rule base is shown in Table 1. This rule base allows the development of a robust thresholding algorithm based on image characteristics. By utilizing fuzzy logic, rules can be created that are not dependent on *exact* measurements of the characteristics, thus allowing *robust* thresholding.

Table 1. The rule base

Mask_Center	Num_Non-Dark Pixels	Mult_Factor
Center	Low	Low
Center	Med	Med
Center	High	Med
NOTCenter	Low	Med
NOTCenter	Med	High
NOTCenter	High	High

Given these membership functions for the image characteristics and the derived fuzzy rule-base, we tested our approach on masks imaged at different sun angles. The images shown in Figure 7 display the extracted mask and the corresponding output from dynamic thresholding.

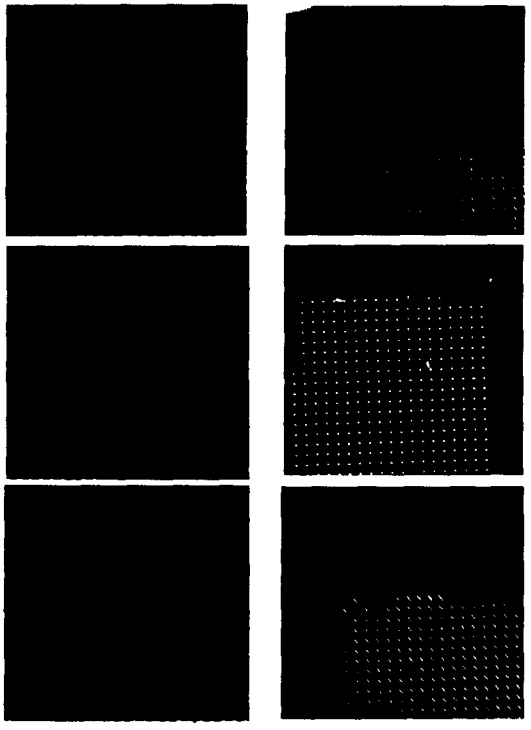

Figure 7: Fuzzy logic thresholding

The fuzzy threshold image from Figure 5 is shown in Figure 8.

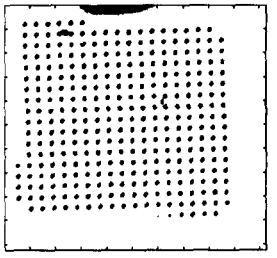

Figure 8: The Fuzzy threshold image of Figure 5

The result of the Fuzzy image thresholding centroiding algorithm is shown in Figure 9. The centroids are shown with a +. Note that the Fuzzy logic algorithm has identified a number of "false" apertures that the conventional algorithm did not find. These extra centroids are not critical, because they do not match any apertures and therefore they will be ignored in the further processing.

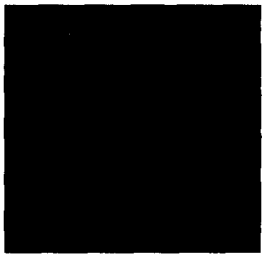

Figure 9: Calculated centroids using Fuzzy thresholding

To evaluate the Fuzzy logic algorithm, a sensor model is developed to determine the overall accuracy of the sun sensor.

V. SENSOR MODEL

The sensor model is a mathematical equation that relates centroid coordinates to the orientation of the sun in an instrument based coordinate system. The sensor model can be used to evaluate the accuracy of the sun sensor.

JPL's Celestial Simulator facility was used to test the sun sensor prototype. The facility contains a Heliostat, which is simply a "sun tracker". The heliostat consists of a large mirror mounted on a two-axis gimbal inside a dome attached to the facility. The sun is tracked using this gimbal system and the sun bundle is directed toward a fixed mirror located on the ceiling of the facility. The end result of all this is that there is a 3 foot diameter sun "bundle" in the middle of the room inside the facility for about 4-6 hours around noon time (depending on the season). A picture of the heliostat is shown in Figure 10.

he 2-axis gimbal is rotated though a large number of different angles and the aperture centroids are recorded. Based on all these measurements it is possible to derive the relationship between the centroids and the sun angles. A

sketch of the 2-axis gimbal with the sun sensor is shown in Figure 11. The dashed lines indicate the two axis of rotation.

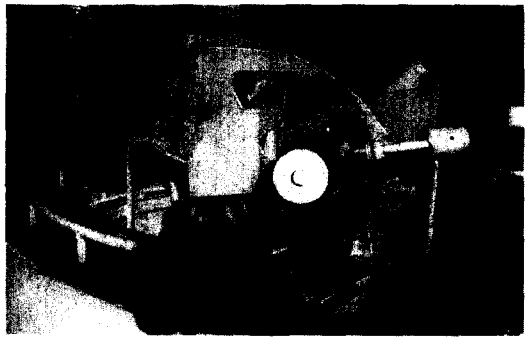

Figure 10: The Heliostat at JPL

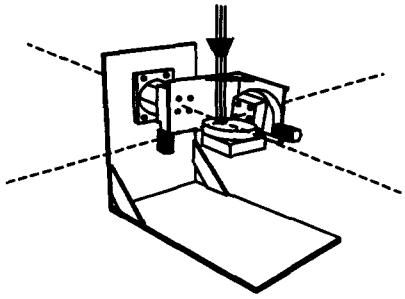

Figure 11: A sketch of the 2-axis gimbal used to calibrate the sun sensor

Only a single aperture centroid has been investigated in this paper. The described procedure has to be applied to all apertures simultaneously in the future. The single aperture that was evaluated was chosen randomly and is shown in Figure 12 with a +.

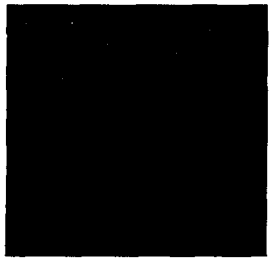

Figure 12: The single aperture that is characterized in this paper is indicated with a +

The gimbal was slewed from –32° to +28° in steps of 4° in one axis and from –40° to +40° in steps of 4° in the other axis. This was a total of 336 images at different orientations. Since one gimbal axis is located on the other gimbal axis, the pattern that the aperture will sweep over on the focal plane is not symmetric (this is counter intuitive to most people). In Figure 13 is shown the positions of the red aperture in Figure 12 over the 336 images.

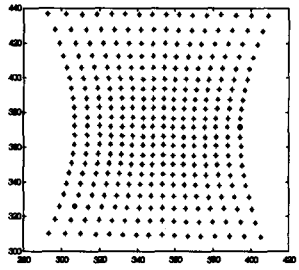

Figure 13: Position of the aperture centroid on focal plane

The sensor model is a simple pinhole camera model. The pinhole model consists of 6 parameters that are the focal length (F), the intersection of boresight with the focal plane (x_0,y_0), and the rotation from the focal plane coordinate system to the external coordinate system (3 different Euler angles, α, β, φ) [7]. It can be shown that the equations from mapping from gimbal angles to centroid coordinates are:

$$\begin{pmatrix} x \\ y \end{pmatrix} = \begin{pmatrix} F \cdot \frac{\tan(\beta-\beta_0)}{\cos(\alpha-\alpha_0)} \cdot \cos\phi - F \cdot \tan(\alpha-\alpha_0) \cdot \sin\phi - x_0 \\ -F \cdot \frac{\tan(\beta-\beta_0)}{\cos(\alpha-\alpha_0)} \cdot \sin\phi - F \cdot \tan(\alpha-\alpha_0) \cdot \cos\phi - y_0 \end{pmatrix} \quad (2)$$

During the data acquisition, 336 measurements were performed. This vector set of angles is called α and β. For each measurement, a set of observed (x, y) centroids on the focal plane was also observed. The four vectors are:

$$\overline{\alpha} = \begin{pmatrix} \alpha_1 \\ \alpha_2 \\ \cdot \\ \alpha_{336} \end{pmatrix} \quad \overline{\beta} = \begin{pmatrix} \beta_1 \\ \beta_2 \\ \cdot \\ \beta_{336} \end{pmatrix} \quad \overline{x_m} = \begin{pmatrix} x_{m,1} \\ x_{m,2} \\ \cdot \\ x_{m,336} \end{pmatrix} \quad \overline{y_m} = \begin{pmatrix} y_{m,1} \\ y_{m,2} \\ \cdot \\ y_{m,336} \end{pmatrix} \quad (3)$$

There are only 6 unknowns. They are α_0, β_0, φ, x_0, y_0 and F. We want to find a solution that minimizes the squared distance between the calculated and measured aperture centroids. Therefore, we want to minimize the following:

$$\sum_{i=1}^{336} \left(F\frac{\tan(\beta_i-\beta_0)}{\cos(\alpha_i-\alpha_0)}\cos\phi - F\tan(\alpha_i-\alpha_0)\sin\phi - x_0 - x_{m,i}\right)^2 + \left(-F\frac{\tan(\beta_i-\beta_0)}{\cos(\alpha_i-\alpha_0)}\sin\phi - F\tan(\alpha_i-\alpha_0)\cos\phi - y_0 - y_{m,i}\right)^2 \quad (4)$$

This can be solved utilizing Matlab or the Solver in Excel.

This equation was solved using centroid estimates from the Fuzzy image algorithm.

The following optimal parameters were found for the Fuzzy logic approach:

$$\begin{aligned} x_0 &= 352.08 \quad F = 907.7\mu \quad \alpha_0 = -1.25° \\ y_0 &= 369.54 \quad \phi = 0.808° \quad \beta_0 = 1.26° \end{aligned} \quad (5)$$

The average error for the solution was found to be 0.166 pixels. The average error is found as the average distance between the measurements and the sensor model (6).

$$\frac{1}{336}\sum_{1}^{336}\sqrt{\left(F\frac{\tan(\beta_i-\beta_0)}{\cos(\alpha_i-\alpha_0)}\cos\phi - F\tan(\alpha_i-\alpha_0)\sin\phi - x_0 - x_{m,i}\right)^2 + \left(-F\frac{\tan(\beta_i-\beta_0)}{\cos(\alpha_i-\alpha_0)}\sin\phi - F\tan(\alpha_i-\alpha_0)\cos\phi - y_0 - y_{m,i}\right)^2} \quad (6)$$

VI. SUMMARY

A new type of sun sensor based on MEMS technology has been described in this paper. A tiny gold and chrome plated silicon wafer is placed at a distance of 900 microns from an APS chip. The mask consists of hundreds of apertures. The sun angle can be determined based on the position of the aperture centroids – just like a sundial.

A new approach utilizing Fuzzy image processing for thresholding is used to calculate centroids. The camera is rotated though a large number of known angles in a calibration setup. Using the pinhole camera model, the centroid data is fitted to the calibration data. These calculations yield an average accuracy of 0.166.

Fuzzy logic has improved the accuracy of the sun sensor. Also, Fuzzy image thresholding has shown the potential of finding centroids at large sun angles where conventional centroid algorithms would not be able to operate. This means that the field of view of the sun sensor can be increased using the Fuzzy image thresholding.

ACKNOWLEDGEMENT

The research described here was carried out at the Jet Propulsion Laboratory, California Institute of Technology, and was sponsored by the National Aeronautics and Space Administration. References herein to any specific commercial product, process or service by trademark, manufacturer, or otherwise, does not constitute or imply its endorsement by the United States Government or the Jet Propulsion Laboratory, California Institute of Technology.

REFERENCES

[1] James R. Wertz: Spacecraft Attitude Determination and Control, D.Reidel Publishing Company, Dordrecht, Holland.

[2] TNO TPD, Netherlands:
http://www.tpd.tno.nl/TPD/smartsite88.html
Cited August 16, 2001.

[3] Ninomiya, Keiken; Ogawara, Yoshiaki; Tsuno, Katsuhiko; Akabane, Satoshi: High accuracy sun sensor using CCDs, AIAA Guidance, Navigation and Control Conference, Minneapolis, MN, Aug. 15-17, 1988, Technical Papers. Part 2 (A88-50160 21-08). Washington, DC, American Institute of Aeronautics and Astronautics, 1988, pp.1061-1070.

[4] Kouzmin, Vladimir S; Cheremoukhin, Gennadi S; Fedoseev, Victor I: Miniature sun sensor, SPIE Proceedings. Vol. 2739, 1996, pp. 407-410.

[5] Z. Zhou, B.Pain and E.R.Fossum: CMOS active pixel sensor with on-chip successive approximation analog-to-digital converter, special issue on Solid-state Image Sensors, IEEE Transactions On Electron Devices, vol. 44 (10), 1997, pp. 1759-1763.

[6] Zadeh, L.A.: "Fuzzy Sets", Information and Control Journal, vol. 12, 1965, pp. 338-353.

[7] C.C.Liebe, S. Mobasser: MEMS based sunsensor: Proceedings of IEEE 2001 Aerospace conference.